

## Design, Synthesis, and Docking Studies of Novel Benzimidazoles for the Treatment of Metabolic Syndrome

Cassia S. Mizuno,<sup>†</sup> Amar G. Chittiboyina,<sup>\*,†</sup> Falgun H. Shah,<sup>†</sup> Akshay Patny,<sup>†</sup> Theodore W. Kurtz,<sup>||</sup> Harrihar A. Pershadsingh,<sup>⊥</sup> Robert C. Speth,<sup>#,∇</sup> Vardan T. Karamyan,<sup>#,○</sup> Paulo B. Carvalho,<sup>†</sup> and Mitchell A. Avery<sup>\*,†,‡,§,∇</sup>

<sup>†</sup>Department of Medicinal Chemistry, School of Pharmacy, <sup>‡</sup>National Center for Natural Products Research, <sup>§</sup>Department of Chemistry & Biochemistry, The University of Mississippi, University, Mississippi 38677, <sup>||</sup>Department of Laboratory Medicine, University of California, San Francisco, California 94122, <sup>⊥</sup>Department of Family Medicine, University of California, Irvine, California 92668, <sup>#,</sup>Department of Pharmacology, University of Mississippi, University, Mississippi 38677-1848, and <sup>∇</sup>Research Institute of Pharmaceutical Sciences, School of Pharmacy, University of Mississippi, University, Mississippi 38677. <sup>○</sup>Present address: Department of Pharmaceutical Sciences, School of Pharmacy, Texas Tech University, Amarillo, Texas 79106.

Received August 25, 2009

In addition to lowering blood pressure, telmisartan, an angiotensin (AT<sub>1</sub>) receptor blocker, has recently been shown to exert pleiotropic effects as a partial agonist of nuclear peroxisome proliferator-activated receptor  $\gamma$  (PPAR $\gamma$ ). On the basis of these findings and docking pose similarity between telmisartan and rosiglitazone in PPAR $\gamma$  active site, two classes of benzimidazole derivatives were designed and synthesized as dual PPAR $\gamma$  agonist/angiotensin II antagonists for the possible treatment of metabolic syndrome. Compound **4**, a bisbenzimidazole derivative showed the best affinity for the AT<sub>1</sub> receptor with a  $K_i = 13.4$  nM, but it was devoid of PPAR $\gamma$  activity. On the other hand **9**, a monobenzimidazole derivative, showed the highest activity in PPAR $\gamma$  transactivation assay (69% activation) with no affinity for the AT<sub>1</sub> receptor. Docking studies lead to the designing of a molecule with dual activity, **10**, with moderate PPAR $\gamma$  activity (29%) and affinity for the AT<sub>1</sub> receptor ( $K_i = 2.5$   $\mu$ M).

### Introduction

Metabolic syndrome (MetS<sup>a</sup>) is a multifactorial disease that, in spite of the efforts of academia and pharma, remains inadequately treated and debilitates millions of people each year. It is characterized as a cluster of metabolic disorders that includes elevated blood pressure, dyslipidemia, insulin resistance, and central obesity.<sup>1</sup> Thus, individuals with metabolic syndrome are 2–3 times more likely to suffer a cardiovascular event and 5–9 times more likely to have type 2 diabetes.<sup>1–3</sup> Two decades ago, only individuals in industrialized countries were affected, however, today, this syndrome affects people worldwide and has become a major concern for healthcare systems.<sup>4</sup>

The development of multifactorial diseases has challenged medicinal chemists to adopt new strategies in drug discovery. While very successful drugs were discovered through the “one target, one disease” approach, multifactorial diseases such as metabolic syndrome cannot be treated using the same method.

Recently there has been an increased interest in designing drugs that modulate multiple targets simultaneously. The advantages of designed multiple ligands (DML) compared to combination therapy include a more predictable phar-

modynamic and pharmacokinetic profile as a consequence of administering only one drug; better compliance to the therapy<sup>5</sup> and lower risk of drug–drug interactions.<sup>6</sup> Because DML are typically larger and more flexible, it suffers from a poor pharmacokinetics profile which could compromise oral bioavailability.<sup>7</sup> The discovery of the DML occurred mostly in the fields of angiotensin, thromboxane A<sub>2</sub>, cyclooxygenase, histamine, PPARs, serotonin receptors, kinases, and nitric oxide releasing conjugates.<sup>8</sup> One of the first DML targeting hypertension was Omapatrilat, a dual angiotensin converting enzyme (ACE)/neutral endopeptidase (NEP) inhibitor.<sup>8</sup> A dual ACE/NEP inhibitor was expected to produce a synergistic effect in the treatment of hypertension and heart failure. However, the development of Omapatrilat was not further pursued due to the occurrence of severe angioedema in treated patients.

Dual PPAR $\alpha/\gamma$  agonists have shown potential in the treatment of metabolic syndrome. The increased insulin sensitivity seen upon activation of PPAR $\gamma$  and the increased lipid oxidation and anti-inflammatory activities shown by PPAR $\alpha$  agonists are a very attractive combination for the treatment of metabolic syndrome. In addition, the combined activity of a dual agonist is expected to reduce weight gain associated with PPAR $\gamma$  activation through the simultaneous stimulation of lipid oxidation and decreased adiposity seen when PPAR $\alpha$  is activated.

Metaglidase (see Chart 1), a PPAR $\gamma$  partial agonist, is the most advanced insulin sensitizer that is currently in phase III clinical trials. The results of phase II clinical trials showed that metaglidase, a prodrug ester that is rapidly and completely modified in vivo to its free acid form, significantly improved

\*To whom correspondence should be addressed. For A.G.C.: 431 Faser Hall; phone, (662) 915-7555; fax, (662) 915-5638; E-mail, amar@olemiss.edu. For M.A.A.: 417 Faser Hall; phone, (662) 915-5879; fax, (662) 915-5638; E-mail, mavery@olemiss.edu.

<sup>a</sup>Abbreviations: AT<sub>1</sub>R, angiotensin-1 receptor, type I; PPAR, peroxisome proliferator-activated receptor; MetS, metabolic syndrome; DML, designed multiple ligands; ACE, angiotensin converting enzyme; NEP, neutral endopeptidase; MW, microwave; LBD, ligand binding domain.

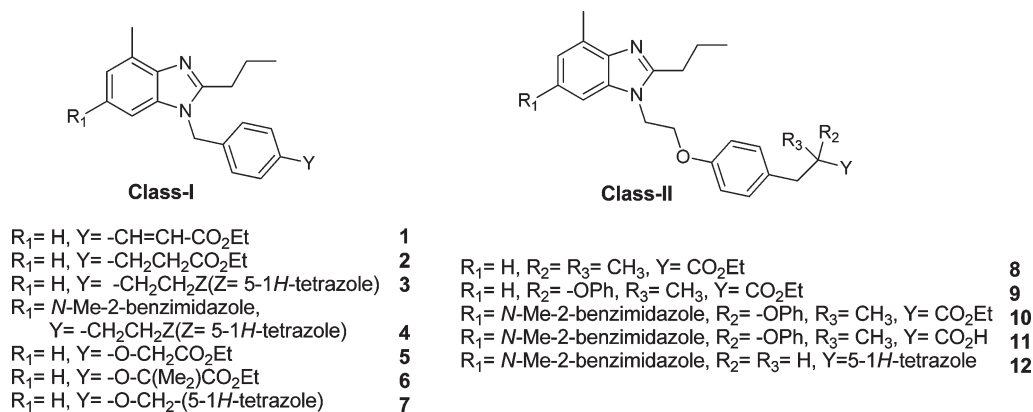
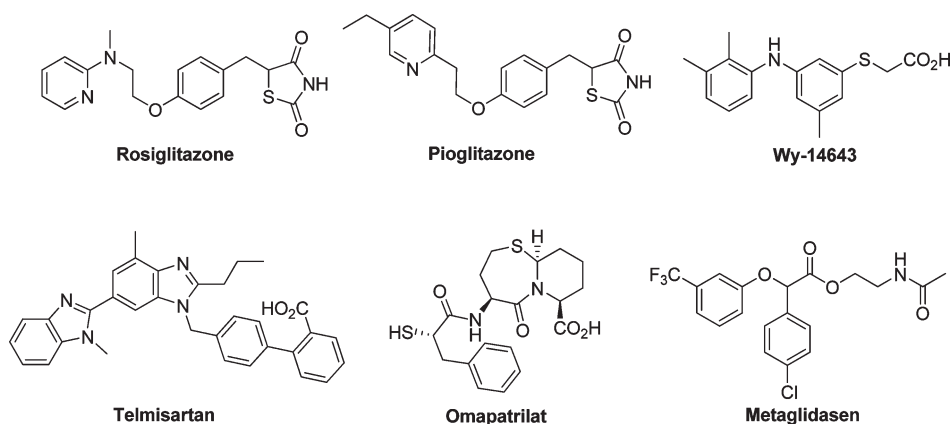


**Figure 1.** Proposed small molecules based on a benzimidazole scaffold.

**Chart 1.** Representative Examples of PPAR Agonists and an ACE Inhibitor



metabolic parameters without the side effects of fluid retention/edema or weight gain.<sup>9</sup>

Rational design of multiple ligands targeting the angiotensin<sup>10–12</sup> system to treat hypertension or PPAR $\gamma$  receptors to treat metabolic disease<sup>13,14</sup> has been successfully attempted; however, these ligands were directed at targets within the same superfamily (e.g., ACE/NEP in the case of hypertension or PPAR $\alpha$ ,  $\gamma$ , and  $\delta$  in the case of metabolic disorders). The design of a multiple ligands targeting two different families of receptors has proven more difficult to achieve.

Currently available antihypertensive drugs were designed with the goal of reducing blood pressure and were not intended to address the association between hypertension and insulin resistance. Therefore, the ability of antihypertensive drugs to ameliorate the metabolic disturbances known to be associated with hypertension is limited.

As part of our ongoing effort to identify small molecule leads for the treatment of metabolic syndrome, we observed that the FDA approved angiotensin antagonist, telmisartan, functioned as a partial PPAR $\gamma$  agonist<sup>15</sup> in a human PPAR $\gamma$ -GAL-4 transactivation assay. These findings provided the framework for the possibility of developing a dual PPAR $\gamma$  agonist/angiotensin II antagonist. Identification of such agents will provide a strategic platform for designing prototypes of a new class of PPAR ligands capable of antagonizing AT1R for broadly targeting cardio-metabolic diseases for which therapy is presently insufficient or nonexistent. Recently, we have made several unsuccessful attempts<sup>16,17</sup> to identify a molecule with such dual activity.

In this work, we have designed and synthesized two classes of benzimidazole-based compounds as potential dual PPAR $\gamma$

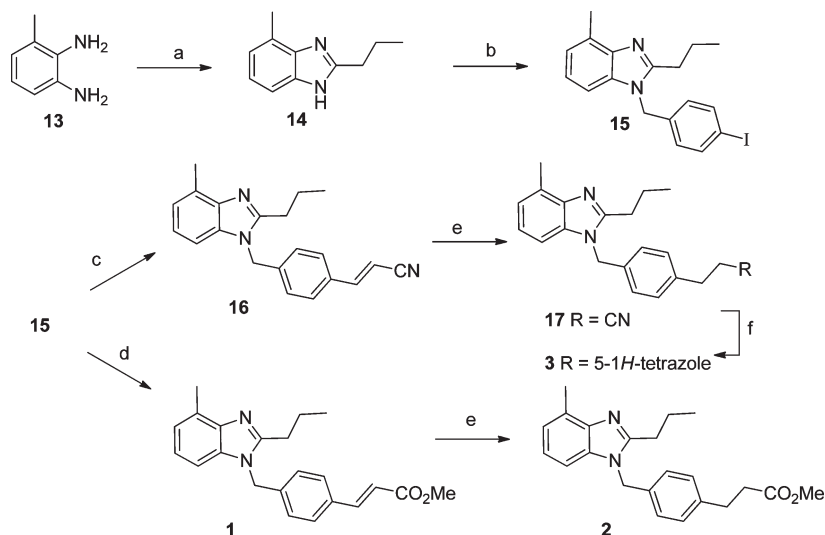
agonists/angiotensin II antagonists (Figure 1). Along with docking studies of the selected derivatives into both PPAR $\gamma$  and AT<sub>1</sub> receptor homology models, their biological activities are also presented.

### Chemistry

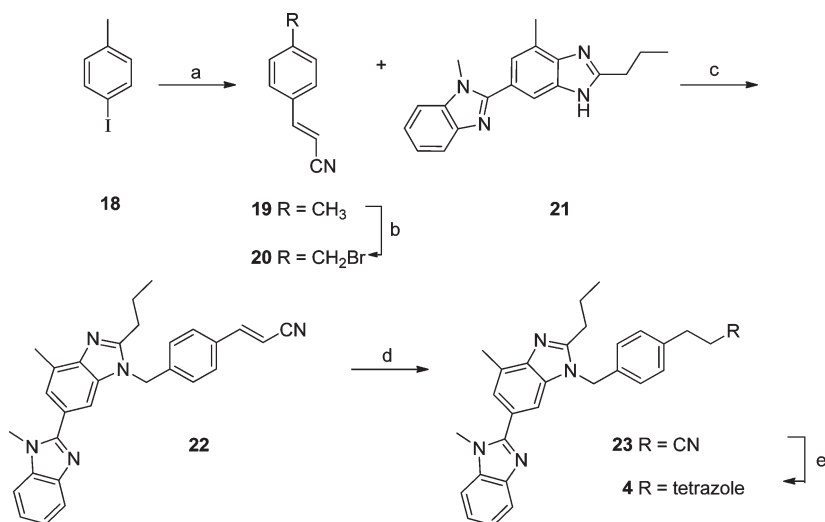
The synthesis of target compounds, 1–3 commenced with the conversion of commercially available 3-methylbenzene-1,2-diamine **13** to benzimidazole **14** using a modified method of Chakravarty et al.<sup>18</sup> where microwave (MW) irradiation was used as an alternative heat source (Scheme 1). Alkylation of benzimidazole **14** with 1-bromo-4-iodobenzene, followed by Heck coupling<sup>19</sup> with acrylonitrile or methylacrylate, gave corresponding compounds **16** and target compound **1**. Hydrogenation of the double bond of **1** and intermediate **16** gave **2** and **17**, respectively. Treatment of the resulting nitrile **17** with sodium azide<sup>20</sup> furnished another target compound **3** in moderate yield.

For SAR studies around the benzimidazole ring, the bisbenzimidazole derivative **4** was designed and synthesized. Compound **19** was obtained via Heck coupling between 4-iodo-1-methylbenzene **18** and acrylonitrile under microwave conditions (Scheme 2). Selective benzylic bromination of **19** with NBS,<sup>21</sup> followed by alkylation with bisbenzimidazole **21**, afforded the required intermediate **22** in good yield (two steps). Selective double bond reduction followed by sodium azide treatment furnished target derivative **4** in moderate yield.

To introduce fibrate-like pharmacophore in designed molecules, compounds **28** and **29** were prepared (Scheme 3). Commercially available *p*-cresol **24** was *O*-alkylated in the

**Scheme 1.** Synthesis of Monobenzimidazole-Based Compounds **1** and **2**

Reagents and conditions: (a) butyric acid, polyphosphoric acid, MW irradiation, 150 °C, 10 min, 57%; (b) 1-bromo-4-iodobenzene, Cs<sub>2</sub>CO<sub>3</sub>, DMF, 60 °C, 3 h, 84%; (c) acrylonitrile, TEA, Pd(OAc)<sub>2</sub>, MW irradiation, 100 °C, 5 min, DMF, 52%; (d) methylacrylate, Pd(OAc)<sub>2</sub>, MW irradiation, TEA, DMF, 60%; (e) Pd/C, H<sub>2</sub>, MeOH, rt, 12 h, 70%; (f) NaN<sub>3</sub>, NH<sub>4</sub>Cl, DMF, 100 °C, 40 h, 52%.

**Scheme 2.** Synthesis of Tetrazole-Based Benzimidazole **4**

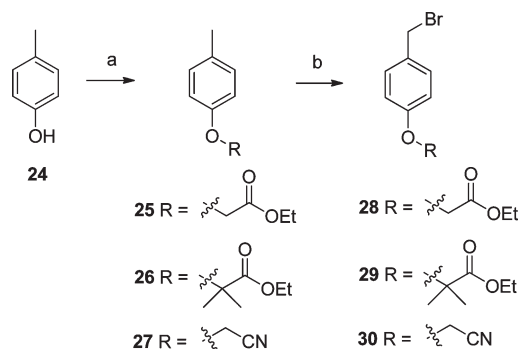
Reagents and conditions: (a) acrylonitrile, TEA, Pd(OAc)<sub>2</sub>, DMF, MW irradiation, 100 °C, 5 min, 96%; (b) NBS, benzoyl peroxide, CCl<sub>4</sub>, reflux, 3 h, 65%; (c) Cs<sub>2</sub>CO<sub>3</sub>, DMF, 60 °C, 3 h, 60%; (d) Pd/C, H<sub>2</sub>, MeOH, rt, 12 h, 71%; (e) NaN<sub>3</sub>, NH<sub>4</sub>Cl, DMF, reflux, 48 h, 50%.

presence of corresponding alkyl bromide and afforded compounds **25**–**27**, respectively. Selective benzylic bromination with NBS followed by *N*-alkylation with benzimidazole **14** yielded corresponding target compounds **5**, **6**, and intermediate **31** (Scheme 4). The intermediate **31** was further subjected to sodium azide conditions to yield required tetrazole derivative **7**.

To study the effects of the spacer between the benzimidazole nitrogen and benzene ring fragments, **36** and **37** were designed and synthesized (Scheme 5).

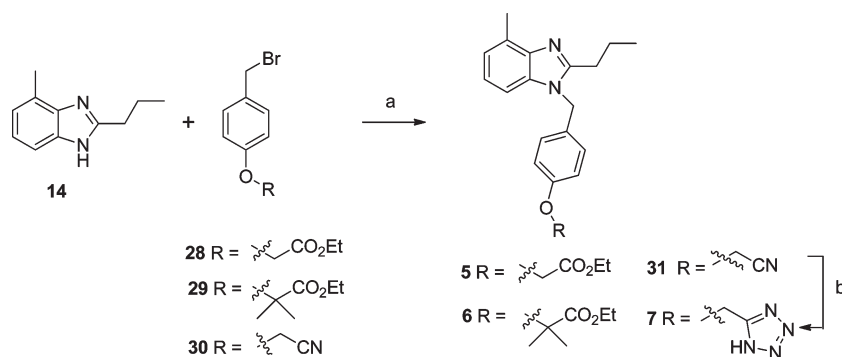
Alkylation of benzimidazole **14** and **21** with ethyl bromoacetate afforded compounds **32** and **33** in good yields. Reduction of esters with LiAlH<sub>4</sub>, followed by mesylation of the corresponding alcohols, gave mesylates **36** and **37** in reasonably good yields.

The synthesis of the second fragment for **8** is depicted in Scheme 6. Condensation of ethyl isobutyrate **38** and benzaldehyde **39** was carried out using LDA in THF.<sup>13</sup> Treatment of

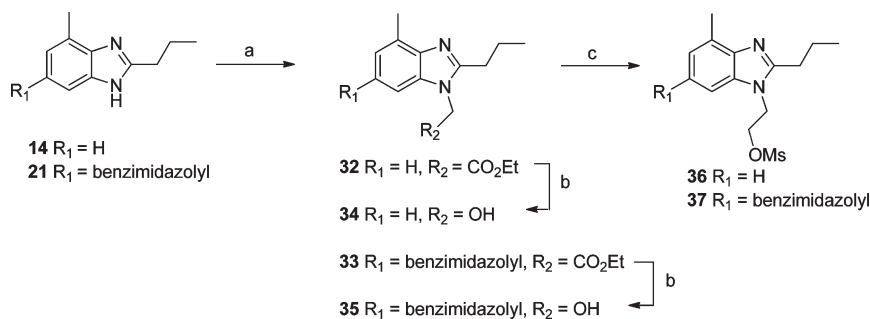
**Scheme 3.** Synthesis of Fibrate-Based Benzimidazoles

Reagents and conditions: (a) ethyl bromoacetate (for **25**), ethyl-2-bromoisobutyrate (for **26**) NaH, THF, 0 °C → rt, 12 h; 2-bromoacetone (for **27**), Cs<sub>2</sub>CO<sub>3</sub>, DMF, 60 °C, 3 h; (b) NBS, benzoyl peroxide, CCl<sub>4</sub>, reflux, 3 h.

## Scheme 4. Benzimidazoles Coupling with Fibrate-like Moieties

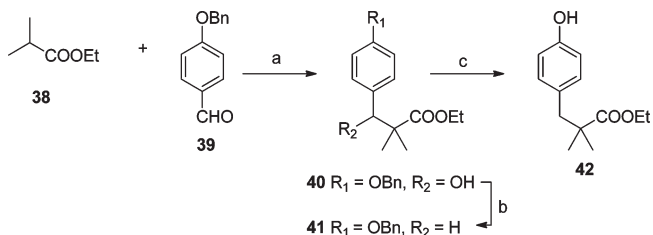


Reagents and conditions: (a)  $\text{Cs}_2\text{CO}_3$ , DMF, 60 °C, 3 h; (b)  $\text{NaN}_3$ ,  $\text{NH}_4\text{Cl}$ , THF, reflux, 3 h, 90 °C, 31%.

Scheme 5. *N*-Substituted Mono(bis)-benzimidazoles

Reagents and conditions: (a) ethyl bromoacetate, NaH, THF, 0 °C, 12 h; (b)  $\text{LiAlH}_4$ , THF, 0 °C, 30 min; (c) MsCl, TEA, DCM, rt, 12 h.

## Scheme 6. Synthesis of 4-Substituted Phenol Fragments



Reagents and conditions: (a) LDA, THF,  $-78\text{ }^\circ\text{C} \rightarrow \text{rt}$ , 66%; (b)  $\text{BF}_3 \cdot \text{Et}_2\text{O}$ ,  $\text{Et}_3\text{SiH}$ , DCM, rt, 2 h, 90%; (c) Pd/C, EtOAc, rt, 12 h, 93%.

**40** with deoxygenation conditions,<sup>22</sup> followed by hydrogenolysis, furnished the required phenol derivative in 55% yield (for three steps).

Coupling of benzimidazole **36** with fragment **42** and **43** under basic conditions (Scheme 7) furnished **8** and **9**, respectively. On the other hand, coupling of bisbenzimidazole **37** and fragment **43** afforded another target compound **10** in moderate yield. Hydrolysis of ester in **10** using alkaline methanol gave the corresponding acid **11** as shown in Scheme 8.

For comparison purposes, the length of **4** was increased to result bisbenzimidazole derivative **12** (Scheme 9). Heck reaction of 4-iodophenol **44** with acrylonitrile, coupled with bisbenzimidazole **37**, afforded the required intermediate **46**. Reduction of the resulting double bond, followed by tetrazole formation, afforded another target compound **12**.

## Results and Discussion

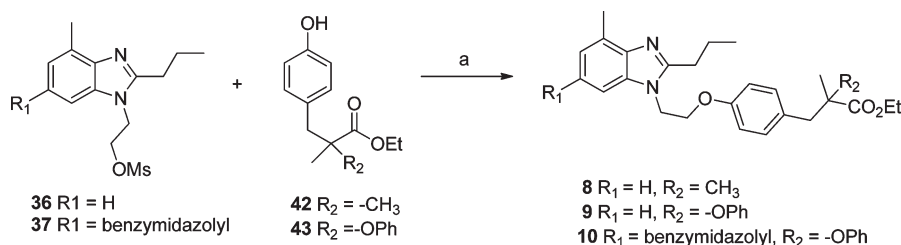
The binding affinity of the compounds for  $\text{AT}_1$  receptors was measured by their ability to compete with  $^{125}\text{I}$ -sarcosine,<sup>1</sup> isoleucine,<sup>8</sup> angiotensin II ( $^{125}\text{I}$ -SI Ang II) binding to rat liver

membranes. All samples were evaluated for the activation of  $\text{PPAR}\gamma$  using the human  $\text{PPAR}\gamma$ -GAL-4 cell-based transactivation assay. The results are summarized in Table 1.

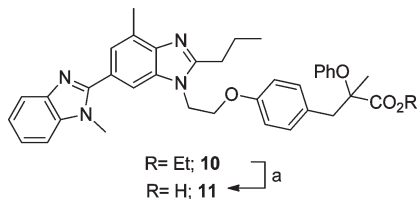
Surprisingly, the compound that showed the best results in an  $\text{AT}_1\text{R}$  radioligand binding assay (**4**,  $K_i = 13.4\text{ nM}$ ) was inactive in a  $\text{PPAR}\gamma$  transactivation assay, whereas the compound **9** was found to be superior in  $\text{PPAR}\gamma$  activity (69%), was inactive in an  $\text{AT}_1\text{R}$  radioligand binding assay.

To explore the structure–activity relationship (SAR) of this series, we synthesized several telmisartan-like analogues with mono- and bis-benzimidazole moieties with different acidic (tetrazole, carboxylate) substitutions. Several structural features necessary for  $\text{AT}_1\text{R}$  affinity as well as  $\text{PPAR}\gamma$  agonist activity were revealed in the present study. The tetrazole containing molecules, **3**, **4**, **7**, and **12** showed better activity in an  $\text{AT}_1\text{R}$  radioligand binding assay compared to corresponding acid and ester analogues. This is further supported by comparing the binding affinities of ester analogue, **2** ( $\text{IC}_{50} > 10\text{ }\mu\text{M}$ ), and corresponding tetrazole analogue, **3** ( $K_i = 2.84\text{ }\mu\text{M}$ ). The same trend was observed when the activities of fibrate-like derivatives [**5** and **6** ( $\text{IC}_{50} > 10\text{ }\mu\text{M}$ )] were compared to the tetrazole analogue, **7** ( $K_i = 5.06\text{ }\mu\text{M}$ ). In contrast to their good affinity toward  $\text{AT}_1\text{R}$ , unfortunately, the compounds **3**, **4**, **7**, and **12** found to be inactive in the  $\text{PPAR}\gamma$  transactivation assay.

In the monobenzimidazole series, elongation of the spacer between the nitrogen of the proximal benzimidazole moiety and aryl ring by three atoms did not improve the affinity for the  $\text{AT}_1$  receptor. For example, compounds **6** with one methylene and **8** with 2 methylenes and one oxygen spacer were inactive in  $\text{AT}_1\text{R}$  assay, whereas the same compounds showed moderate activity against  $\text{PPAR}\gamma$ . Another interesting key feature of the current SAR study is where derivatives

Scheme 7. Synthesis of  $\alpha$ -Aryloxy-carboxy Benzimidazoles 8–10

Reagents and conditions: Cs<sub>2</sub>CO<sub>3</sub>, DMF, 60 °C, 3 h.

Scheme 8. Synthesis of  $\alpha$ -Aryloxy Carboxy Benzimidazoles 10 and 11

Reagents and conditions: (a) KOH, MeOH, rt, 24 h.

bearing bisbenzimidazole moiety showed better activity in AT<sub>1</sub>R than the corresponding monobenzimidazoles. This result is supported by the comparison of AT<sub>1</sub>R affinities of monobenzimidazoles **3** ( $K_i = 2.84 \mu\text{M}$ ) and **9** ( $\text{IC}_{50} > 10 \mu\text{M}$ ) with bisbenzimidazole derivatives **4** ( $K_i = 13 \text{ nM}$ ) and **10** ( $K_i = 2.53 \mu\text{M}$ ). These results further suggest that bisbenzimidazole unit is crucial pharmacophore for maintaining AT<sub>1</sub> affinity.

Docking studies were performed to evaluate the binding mode of compounds in AT<sub>1</sub>R using a homology model<sup>23</sup> and rosiglitazone-bound crystal structure for PPAR $\gamma$  (PDB code: 2PRG) (Figure 2). Previous SAR and mutation studies revealed His 256, Asn 111, Asn 295, and Lys 199 as key amino acid residues for the binding of AT<sub>1</sub>R antagonists.<sup>24–26</sup> For PPAR $\gamma$ , interactions with key polar residues near AF-2 helix, Tyr 473, His 449, and His 323 are crucial for full activation of the receptor,<sup>27</sup> whereas several hydrophobic interactions mainly with residues of H3, H6, and H7 helices, accounts for partial activation.<sup>28</sup>

The bisbenzimidazole analogue, **4**, displayed potent binding affinity for the AT<sub>1</sub>R ( $K_i = 13.4 \text{ nM}$ ). The compound **4** also showed all key interactions important for AT<sub>1</sub>R affinity as depicted in docking studies. As shown in Figure 3, the nitrogen on the distal benzimidazole ring of **4** interacts with N( $\delta$ ) of His 256 through hydrogen bonding within a distance of 1.7 Å. Additionally, the acceptor nitrogen atom of the proximal heterocyclic benzimidazole ring of **4** formed a hydrogen bond (H-bond) with Asn 111 and Asn 295 with a distance of 2.5 Å and 2.2 Å, respectively. Also, free rotation of the tetrazole moiety in the active site (linked by two methylene units to a phenyl ring) helped to attain a favorable conformation to form an ionic bond with Lys 199 with a distance of 2.3 Å, an important interaction for AT<sub>1</sub> affinity.

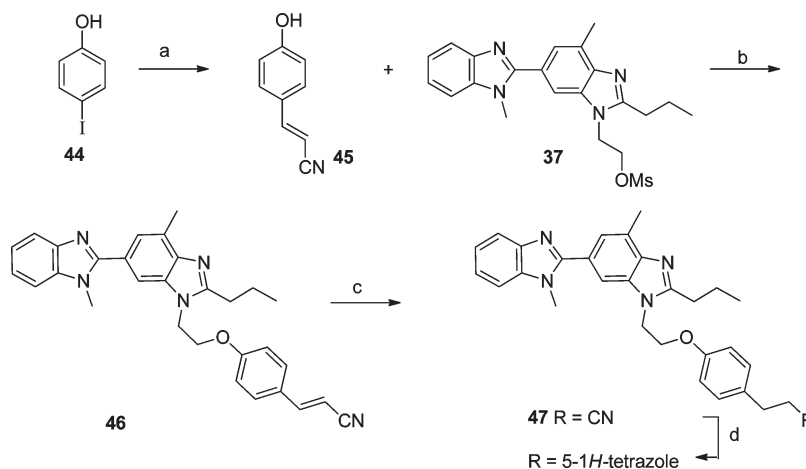
The presence of these interactions with key residues of AT<sub>1</sub>R active site explains the potency of **4** in binding assay. However, the compound **4** was inactive in the PPAR $\gamma$  transactivation assay. This result was in agreement with the recent findings reported by Goebel et al.,<sup>29</sup> where introduction of a second benzimidazole group to monobenzimidazole compound diminished the PPAR $\gamma$  activation. To explain the inactivity of **4**, the benzimidazole derivative was docked into

PPAR $\gamma$  ligand binding domain as shown in Figure 4. From the docking pose, it is evident that the short length of the phenethyl tetrazole arm, and as a result, lack of interactions with key residues near AF-2 helix, might be responsible for the inactivity of **4** in the PPAR $\gamma$  transactivation assay.

Elongation of compound **4** with one methylene and one oxygen spacer between the nitrogen from the benzimidazole and the aromatic ring yielded **12**. The resultant compound displayed moderate binding affinity for the AT<sub>1</sub>R ( $K_i = 1.62 \mu\text{M}$ ). The possible explanation for a lower affinity of **12** compared to telmisartan ( $K_i = 0.23 \text{ nM}$ ) and **4** in AT<sub>1</sub>R might be a loss of the key interaction of tetrazole with Lys199 as shown in Figure 3. Other H-bonding interactions with Asn 195, Asn 111, and His 256 were retained. Docking studies of **12** in PPAR $\gamma$  (shown in Figure 4) depicted H-bond interaction with backbone NH of Ser 342 residue. Also, the center phenyl ring of **12** exhibited Van der Waals interactions with Cys 285 and Leu 330. The loss of key interactions in AF-2 helix might be one of the reasons for the loss of its PPAR $\gamma$  activity.

The compound **9** showed the best result in the PPAR $\gamma$  assay with an activation of 69% and an EC<sub>50</sub> of 2.3  $\mu\text{M}$  (pioglitazone EC<sub>50</sub> = 0.9  $\mu\text{M}$ ) as a partial agonist. When tested against other isoforms of PPAR, **9** showed an EC<sub>50</sub> of 0.3  $\mu\text{M}$  (WY 14643 EC<sub>50</sub> = 0.7  $\mu\text{M}$ ) with 93% activation in PPAR $\alpha$  as a full agonist, whereas in PPAR $\delta$  did not show any activity. Thus, the phenoxy derivative **9** found to be a dual PPAR $\alpha/\gamma$  agonist. To study the effect of stereochemistry of compounds **9** and **10**, we have undertaken docking studies of both *R* and *S* isomers in AT<sub>1</sub> and PPAR $\gamma$  receptor. In the case of compound **9**, the *R* isomer showed reasonable interactions with residues near AF2 helix. Figure 5 shows the proposed binding mode of *R*-isomer of **9** in the PPAR $\gamma$  LBD. The benzimidazole acceptor nitrogen atom forms a H-bond with the Ser 342 residue at a distance of 2 Å. The phenoxy moiety of *R* isomer of **9** displayed a H-bond with His 323, and furthermore it was stabilized by hydrophobic interactions with Cys 285, Leu330, Phe 363, and Tyr 473. These favorable interaction profiles of **9** in the PPAR $\gamma$  LBD may explain its higher activity in PPAR $\gamma$  transactivation assay.

In the AT<sub>1</sub>R model, docking of **9** (Figure 6) revealed the absence of key interactions with His 256. The molecular modeling studies suggested that the lack of affinity of **9** for the AT<sub>1</sub>R might be due to the absence of a second (distal) benzimidazole ring. Therefore, we designed a new compound by appending a second benzimidazole ring to monobenzimidazole **9**. The resultant compound **10** exhibited moderate affinity (2.53  $\mu\text{M}$ ) for the AT<sub>1</sub>R as anticipated. As shown in Figure 7, the interaction of the distal benzimidazole moiety with His 256 helped to regain affinity for the angiotensin receptor. The proximal benzimidazole ring showed H-bond interactions with Asn 295 and Asn 111. In addition, phenyl

Scheme 9. Synthesis of Tetrazole-Based Bisbenzimidazole **12**

Reagents and conditions: (a) acrylonitrile, TEA, Pd(OAc)<sub>2</sub>, MW irradiation, 100 °C, 5 min, DMF, 96%; (b) Cs<sub>2</sub>CO<sub>3</sub>, DMF, 60 °C, 3 h, 96%; (c) Pd/C, EtOAc, rt, 12 h, 93%; (d) NaN<sub>3</sub>, NH<sub>4</sub>Cl, DMF, 100 °C, 40 h, 22%.

**Table 1.** Biological Results of Novel Bisbenzimidazoles for PPAR $\gamma$  and AT<sub>1</sub>R

compd	AT <sub>1</sub> R K <sub>i</sub> ± SEM (nM) <sup>a</sup>	% of maximum PPAR $\gamma$ activation at 10 $\mu$ M <sup>b</sup>
<b>1</b>	> 10000	4
<b>2</b>	> 10000	2
<b>3</b>	2840 ± 272	
<b>4</b>	13.4 ± 4.6	
<b>5</b>	> 10000	
<b>6</b>	> 10000	21
<b>7</b>	5060 ± 1023	
<b>8</b>	> 10000	10
<b>9</b>	> 10000	69 (93) <sup>c</sup>
<b>10</b>	2534 ± 661	29 (15) <sup>c</sup>
<b>11</b>	2226 ± 149	12
<b>12</b>	1618 ± 27	
telmisartan	0.23 ± 0.09	21.9

<sup>a</sup> Values > 10000 are IC<sub>50</sub> values. <sup>b</sup> % of maximum PPAR $\gamma$  activation achieved by full agonist. <sup>c</sup> Number in parentheses represents for % of maximum PPAR $\alpha$  activation achieved with full agonist at 10 mM.

side chain of **10** exhibited the additional  $\pi$ - $\pi$  interactions with Phe 261 (not shown), which might account for its modest affinity toward AT<sub>1</sub>R. However, both enantiomers of **10** did not show any interaction with key Lys 199 residue in our docking studies (Figure 8).

Compound **10** exhibited lower activity (29.6%) in the PPAR $\gamma$  transactivation assay compared to the parent compound **9** (69%). One possible explanation for the lower activity of **10** might be improper placement of the distal benzimidazole moiety in the downward arm of the distal hydrophobic pocket which might interfere with proper folding of the PPAR $\gamma$  receptor necessary for activation. Both enantiomers of **10** are mainly stabilized by hydrophobic interactions with the residues (Cys 285, Leu 330, Phe 363, and Tyr 473) of PPAR $\gamma$  LBD with no polar interactions with residues near AF-2 helix. Tagami et al.<sup>30</sup> have studied the difference on the transcriptional control between telmisartan and thiazolidinediones using PPAR $\gamma$  mutants. Thus, it was observed that the activation of the receptor by thiazolidinediones was impaired in the H323Y, S342A, H449A, and Y473A mutants. However, activation stimulated by telmisartan was retained in all four mutants, and in the Y473A mutant, the activation

was greater than thiazolidinedione-induced activation. On the basis of this study, **10** may have the same effects on the transcriptional control as telmisartan showing moderate activation of the receptor without directly interacting with the residues near AF-2 helix, important for full activation of the receptor. In addition, **10** also showed modest activity in the PPAR $\alpha$  assay (15% activation).

Hydrolysis of the ester in **10** gave the corresponding acid derivative **11**, which did not have a major effect on binding affinity toward the AT<sub>1</sub>R because the carboxylic acid analogue, **11** (K<sub>i</sub> = 2.23  $\mu$ M) exhibited affinity close to that of the parent ester analogue **10** (K<sub>i</sub> = 2.53  $\mu$ M). However, this acid analogue was completely devoid of PPAR $\gamma$  activity.

## Conclusion

In summary, we have discovered a dual angiotensin II antagonist/PPAR $\gamma$  agonist molecule **10**. In addition to the dual activity, the benzimidazole derivative **10** also exhibited moderate activity against PPAR $\alpha$ . Despite the weaker binding affinity of **10** in AT<sub>1</sub>R, its additional PPAR $\alpha$  activity makes it useful starting point for design of multiple ligands. During the course of this work, significantly active nonpeptide AT<sub>1</sub> antagonist, **4**, was synthesized together with a PPAR $\alpha$ / $\gamma$  dual agonist **9**. Efforts to increase PPAR $\gamma$  activity of AT<sub>1</sub> antagonist **4** was found to be unsuccessful. However, modification of dual PPAR  $\alpha$ / $\gamma$  activator **9** generated another interesting compound **10**, with moderate activity against PPAR $\alpha$ , PPAR $\gamma$ , and AT<sub>1</sub> receptor. Thus, the multiple activity of **10** at AT<sub>1</sub> receptor and PPAR $\alpha$ / $\gamma$  suggests that phenoxy benzimidazole **10** can be used as a starting point for the development of multiple AT<sub>1</sub>R antagonists and PPAR $\alpha$ / $\gamma$  agonists for the treatment of multifactorial disorders such as metabolic syndrome. To achieve dual activity against PPAR $\gamma$  and AT<sub>1</sub> R, further efforts for the structural modifications of **10** are currently underway according to insights gained from the present study.

## Experimental Section

**Materials and Methods.** All solvents that could not be bought anhydrous were distilled and/or stored with molecular sieves or sodium prior to utilization. All reactions were run under an inert atmosphere unless aqueous. All round-bottom flasks were dried

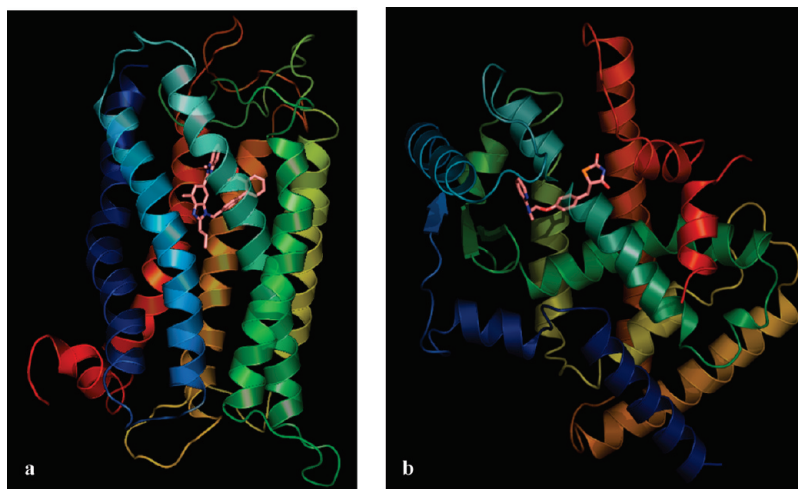


**Figure 2.** (a) Telmisartan-bound AT<sub>1</sub>R homology model; (b) rosiglitazone-bound crystal structure of PPAR $\gamma$  (PDB code: 2PRG).

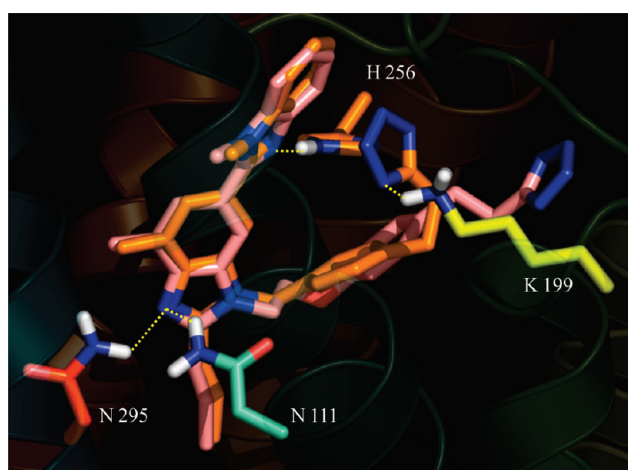


**Figure 3.** The proposed binding mode of **4** and **12** in the AT<sub>1</sub>R homology model. Only key residues of AT<sub>1</sub>R are shown. Hydrogen bonds are denoted as yellow dotted lines. The benzimidazole **4** is shown in orange and **12** is shown in pink (colored by atom types).

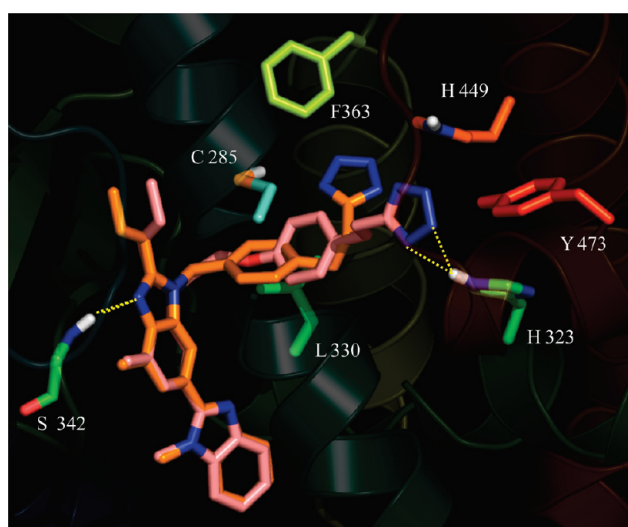


**Figure 4.** The proposed binding mode of **4** and **12** in the PPAR $\gamma$  receptor (PDB code 2PRG). Only important residues of the protein are shown. Hydrogen bonds are denoted as yellow dotted lines. The compound **4** is shown in orange and **12** is shown in pink (colored by atom types).

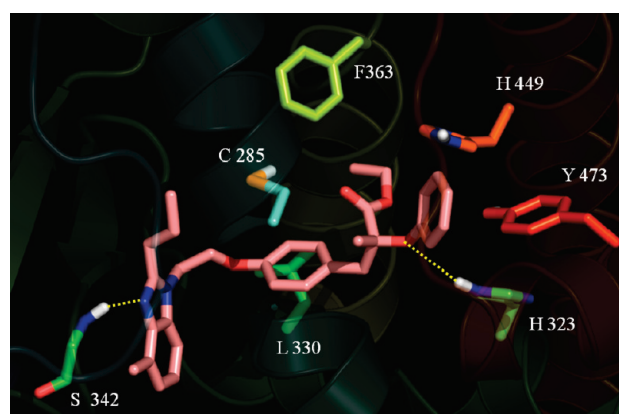


**Figure 5.** The proposed binding mode of the *R* isomer of **9** in the PPAR $\gamma$  (PDB code: 2PRG). Only important residues of PPAR $\gamma$  LBD is shown (colored by atom types). Hydrogen bonds are denoted as yellow dotted lines.

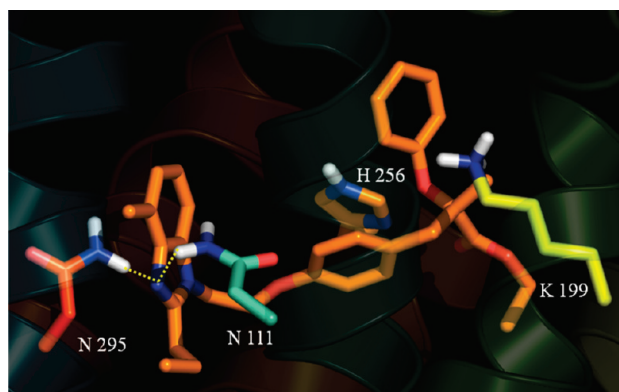


**Figure 6.** The proposed binding mode of *R* isomer of **9** in the AT<sub>1</sub>R homology model with only important residues are shown (colored by atom types). Hydrogen bonds are denoted as yellow dotted lines.

under vacuum and heat prior to use. Melting points were obtained on an OptiMelt capillary melting apparatus. All NMR data were obtained on a Bruker 500 MHz, 400 MHz, or Bruker 400 MHz Ultra Shield and the analyses conducted in CDCl<sub>3</sub>, MeOD, or DMSO-*d*<sub>6</sub>. Flash chromatography was done using silica gel Sorbent Technologies (230  $\times$  400 mesh). IR spectra were obtained on a Bruker Tensor 27. HRMS were obtained on a Waters Micromass Q-TOF micro mass spectrometer, and LCMS were

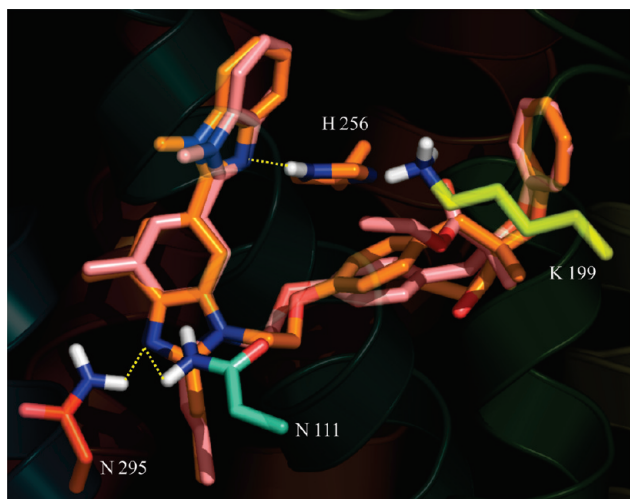


**Figure 7.** The proposed binding mode of *R* and *S* isomers of **10** in the AT<sub>1</sub>R homology model. Only important residues of the AT<sub>1</sub>R are shown. Hydrogen bonds are denoted as yellow dotted lines. *R* and *S* isomer of **10** is shown in pink and orange, respectively (colored by atom types).

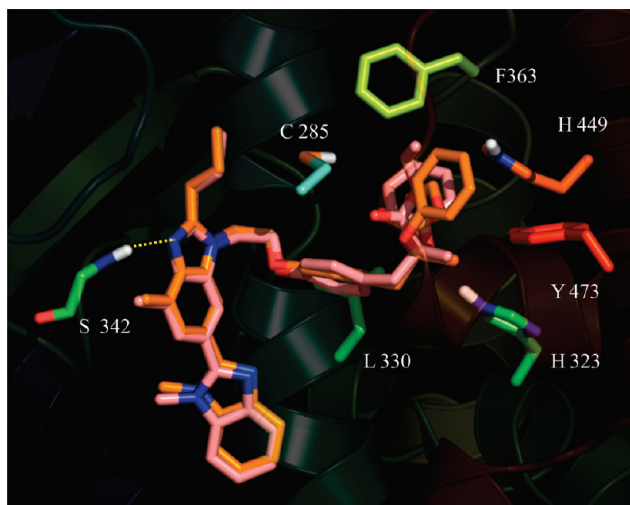


**Figure 8.** The proposed binding mode of the *R* and *S* isomers of **10** in the PPAR $\gamma$  (PDB code: 2PRG). Only important residues of PPAR $\gamma$  LBD are shown. Hydrogen bonds are denoted as yellow dotted lines. The *R* and *S* isomer of **10** is shown in pink and orange, respectively (colored by atom types).

obtained on a Waters AcQuity Ultra Performance LC. Purity of the final compounds ( $\geq 95\%$ ) was established using a Waters HPLC 2695.

**Ethyl 3-(4-((4-Methyl-2-propyl-1*H*-benzo[d]imidazol-1-yl)methyl)phenyl)acrylate (1).** In a 5 mL reaction vial, iodide **15** (0.21 g, 0.53 mmol), methyl acrylate (60  $\mu$ L, 0.66 mmol), Pd(OAc)<sub>2</sub> (catalytic), TEA (74  $\mu$ L, 0.53 mmol), and DMF (500  $\mu$ L) were added. The contents of the flask were irradiated, at 100 °C, 20 psi, and 100 W for 5 min. After cooling, the mixture was poured into water and extracted with DCM. The organic phase was concentrated under vacuum. The resulting crude was purified by silica gel flash chromatography eluting with hexanes:EtOAc (3:2) and provided the target compound **1** in 0.11 g (60% yield). <sup>1</sup>H NMR (CDCl<sub>3</sub>, 400 MHz):  $\delta$  1.01 (t, 3H,  $J = 7.2$  Hz), 1.82 (dd, 2H,  $J_{1,2} = 7.6$  Hz,  $J_{1,3} = 15.2$  Hz), 2.71 (s, 3H), 2.85 (t, 2H,  $J = 8$  Hz), 3.80 (s, 3H), 5.34 (s, 2H), 6.40 (d, 1H,  $J = 16$  Hz), 6.99–7.11 (m, 5H), 7.45 (d, 2H,  $J = 8$  Hz), 7.65 (d, 1H,  $J = 16$  Hz). <sup>13</sup>C NMR (CDCl<sub>3</sub>, 100 MHz):  $\delta$  14.0, 16.7, 21.8, 29.7, 46.8,

51.6, 106.9, 118.2, 122.2, 122.6, 126.6 (2C), 128.5 (2C), 129.3, 134.0, 134.8, 138.4, 141.9, 143.8, 154.4, 167.1. HRMS: calcd for C<sub>22</sub>H<sub>25</sub>N<sub>2</sub>O<sub>2</sub> [M + H] 349.1916, found 349.1910; mp 124.6 °C. IR: 3387, 2961, 1716, 1637, 1207 cm<sup>-1</sup>. UPLC (method 1): 98% pure (1.02 min). UPLC (method 2): 97% pure (0.61 min).

**Methyl 3-(4-((4-Methyl-2-propyl-1*H*-benzo[d]imidazol-1-yl)methyl)phenyl)propanoate (2).** To a solution of acrylate **1** (0.15 g, 0.47 mmol) in MeOH (10 mL) was added catalytic amounts of 10% Pd/C and the reaction mixture was hydrogenated with balloon pressure for overnight at room temperature. The reaction mixture was filtered, and the filtrate was concentrated under vacuum. The residue was purified by flash chromatography over silica gel eluting with CHCl<sub>3</sub>:MeOH (9:1) yielded 0.11 g (70% yield) of **2**. <sup>1</sup>H NMR (CDCl<sub>3</sub>, 400 MHz):  $\delta$  1.01 (t, 3H,  $J = 7.30$  Hz), 1.80 (dd, 2H,  $J_{1,2} = 7.2$  Hz,  $J_{1,3} = 15.2$  Hz), 2.60 (t, 2H,  $J = 7.8$  Hz), 2.05 (s, 3H), 2.86 (t, 2H,  $J = 8.0$  Hz), 2.92 (t, 2H,  $J = 7.5$  Hz), 3.66 (s, 3H), 5.29 (s, 2H), 6.97 (d, 2H,  $J = 7.8$  Hz), 7.01–7.07 (m, 3H), 7.13 (d, 2H,  $J = 7.8$  Hz). <sup>13</sup>C NMR (CDCl<sub>3</sub>, 100 MHz):  $\delta$  14.0, 16.7, 21.8, 29.7, 30.4, 35.4, 46.8, 51.5, 107.0, 122.0, 122.4, 126.3 (2C), 128.8 (2C), 129.1, 134.2, 135.0, 140.1, 141.9, 154.5, 173.0. HRMS: calcd for C<sub>22</sub>H<sub>26</sub>N<sub>2</sub>O<sub>2</sub> [M + H], found 351.2058; mp 66.6 °C. IR: 3387, 2960, 1736, 1514, 1436 cm<sup>-1</sup>. UPLC (method 1): 97% pure (1.05 min). UPLC (method 2): 97% pure (0.61 min).

**General Procedure for Synthesis of 3, 4, 7, and 12.** To a solution of **17** (0.2 g, 0.62 mmol) in DMF (10 mL), NaN<sub>3</sub> (0.16 g, 2.49 mmol) and NH<sub>4</sub>Cl (66.8 mg, 1.24 mmol) were added and the reaction mixture heated to 100 °C. After stirring at 40 h, the suspension was cooled, poured into ice–water, and extracted with EtOAc. The combined organic phases were dried over MgSO<sub>4</sub>, evaporated, and the crude was purified by silica gel column chromatography eluting with chloroform/methanol (9:1) to give **3** in 52% yield. <sup>1</sup>H NMR (CDCl<sub>3</sub>, 500 MHz):  $\delta$  0.93 (t, 3H,  $J = 7.5$  Hz), 1.72 (dd, 2H,  $J_{1,2} = 7.5$  Hz,  $J_{1,3} = 15$  Hz), 2.52 (s, 3H), 2.79 (t, 2H,  $J = 8$  Hz), 3.00 (t, 2H,  $J = 7.8$  Hz), 3.15 (t, 2H,  $J = 8$  Hz), 5.40 (s, 2H), 6.95 (d, 1H,  $J = 7$  Hz), 6.99 (d, 2H,  $J = 8$  Hz), 7.03 (t, 1H,  $J = 7.5$  Hz), 7.16 (d, 2H,  $J = 8$  Hz), 7.21 (d, 1H,  $J = 7.5$  Hz). <sup>13</sup>C NMR (CDCl<sub>3</sub>, 125 MHz):  $\delta$  14.6, 17.2, 21.5, 25.2, 29.4, 33.0, 46.5, 108.1, 121.9, 122.1, 126.8 (2C), 128.2, 128.9 (2C), 135.1, 135.5, 139.4, 141.8, 154.4, 155.6. HRMS: calcd for C<sub>21</sub>H<sub>25</sub>N<sub>6</sub> 361.2141 [M + H], found 361.2132; mp 184.3 °C. IR: 3404, 3204, 2927, 1656, 1606 cm<sup>-1</sup>. UPLC (method 1): 99% pure (0.50 min). UPLC (method 2): 99.4% pure (0.46 min).

**3'-(4-(2-(1*H*-Tetrazol-5-yl)ethyl)benzyl)-1,7'-dimethyl-2'-propyl-1*H*,3'*H*-2,5'-bibenzo[d]imidazole (4).** Yield 50%. <sup>1</sup>H NMR (CDCl<sub>3</sub>, 400 MHz):  $\delta$  1.03 (t, 3H,  $J = 6$  Hz), 1.84 (dd, 2H,  $J_{1,2} = 5.6$  Hz,  $J_{1,3} = 12$  Hz), 2.71 (s, 3H), 2.88–2.91 (m, 2H), 2.98 (t, 2H,  $J = 5.6$  Hz), 3.14 (t, 2H,  $J = 5.2$  Hz), 3.81 (s, 3H), 5.26 (s, 2H), 6.83 (s, 4H), 7.23 (s, 1H), 7.26–7.33 (m, 4H), 7.40 (d, 1H,  $J = 6$  Hz), 7.65 (d, 1H,  $J = 6.4$  Hz). <sup>13</sup>C NMR (CDCl<sub>3</sub>, 100 MHz):  $\delta$  14.4, 17.3, 22.2, 26.0, 30.0, 32.1, 34.1, 47.6, 109.7, 110.0, 118.2, 122.3, 122.9, 123.1, 133.3, 126.4 (2C), 128.8 (2C), 129.4, 133.4, 134.8, 135.8, 139.5, 140.9, 143.21, 154.2, 156.0, 156.6. HRMS: calcd for C<sub>29</sub>H<sub>31</sub>N<sub>8</sub> 491.2672 [M + H], found 491.2687; mp 97 °C. IR: 2962, 2931, 2872, 1653, 1597, 1454, 1417 cm<sup>-1</sup>. UPLC (method 1): 96.3% pure (0.50 min). UPLC (method 2): 97.0% pure (0.53 min).

**1-(4-((1*H*-Tetrazol-5-yl)methoxy)benzyl)-4-methyl-2-propyl-1*H*-benzo[d]imidazole (7).** Yield 31%. <sup>1</sup>H NMR (DMSO, 500 MHz):  $\delta$  0.94 (t, 3H,  $J = 3.6$  Hz), 1.72 (dd, 2H,  $J_{1,2} = 6$  Hz,  $J_{1,3} = 12$  Hz), 2.51 (s, 3H), 2.82 (t, 2H,  $J = 6.4$  Hz), 5.25 (s, 2H), 5.37 (s, 2H), 7.022 (m, 6H), 7.23 (d, 1H,  $J = 6.4$  Hz). <sup>13</sup>C NMR (DMSO, 125 MHz):  $\delta$  14.6, 17.2, 21.5, 29.4, 46.3, 61.0, 108.1, 115.3 (2C), 122.0, 122.1, 128.1 (2C), 129.9 (2C), 135.0, 141.6, 154.4 (2C), 157.5. HRMS: calcd for C<sub>20</sub>H<sub>25</sub>N<sub>6</sub>O 363.1933 [M + H], found 363.1934; mp 104.7 °C. IR: 3382, 2960, 2926, 1662, 1611, 1511 cm<sup>-1</sup>. UPLC (method 1): 99.3% pure (0.51 min); UPLC (method 2): 100% pure (0.47 min).

**3'-(2-(4-(2-(1*H*-Tetrazol-5-yl)ethyl)phenoxy)ethyl)-1,7'-dimethyl-2'-propyl-1*H*,3'*H*-2,5'-bibenzo[d]imidazole (12).** Yield 22%. <sup>1</sup>H NMR (CDCl<sub>3</sub>, 400 MHz):  $\delta$  1.07 (t, 3H,  $J = 7.5$  Hz), 1.91 (dd, 2H,  $J_{1,2} = 7.3$  Hz,  $J_{1,3} = 15.1$  Hz), 2.67 (s, 3H), 2.75 (t, 2H,  $J =$



7.0 Hz), 2.93–3.01 (m, 4H), 3.90 (s, 3H), 4.00 (t, 2H,  $J = 4.5$  Hz), 4.49 (t, 2H,  $J = 4.2$  Hz), 6.28 (d, 2H,  $J = 8.5$  Hz), 6.57 (d, 2H,  $J = 8.3$  Hz), 7.28 (s, 1H), 7.30–7.36 (m, 2H), 7.41–7.43 (m, 1H), 7.76–7.79 (m, 2H).  $^{13}\text{C}$  NMR ( $\text{CDCl}_3$ , 100 MHz):  $\delta$  14.0, 16.9, 21.8, 25.6, 29.4, 31.9, 32.9, 43.6, 65.7, 109.1, 110, 114 (2C), 118.6, 122.6, 123, 123.2, 123.5, 129.1 (2C), 129.3, 132.2, 134.7, 136.1, 141.3, 143.1, 154.5, 156, 156.1, 157.5. HRMS: calcd for  $\text{C}_{30}\text{H}_{33}\text{N}_8\text{O}$  521.2777 [M + H], found 521.2787. IR: 3383, 2962, 2930, 1511, 1454, 1243  $\text{cm}^{-1}$ . UPLC (method 1): 96% pure (0.50 min). UPLC (method 2): 95% pure (0.46 min).

**General Procedure for the Synthesis of 5, 6, 8, 9, and 10.** To a solution of benzimidazole **14** (0.1 g, 0.57 mmol) in 10 mL of DMF was added  $\text{Cs}_2\text{CO}_3$  (0.28 g, 0.85 mmol), the mixture was stirred for 30 min at 60 °C, and ethyl 2-(4-(bromomethyl)phenoxy)acetate **28** (0.15 g, 0.69 mmol) was added. After stirring for 3 h, the mixture was cooled, poured into water, and extracted with EtOAc. The organic phase was dried using  $\text{MgSO}_4$  and evaporated. The residue was purified by silica gel column chromatography eluting with ether/hexanes (7:3) to give 0.14 g (67% yield) of **5**.  $^1\text{H}$  NMR ( $\text{CDCl}_3$ , 400 MHz):  $\delta$  1.01 (t, 3H,  $J = 7.3$  Hz), 1.29 (t, 3H,  $J = 7.1$  Hz), 1.8 (dd, 2H,  $J_{1,2} = 7.6$  Hz,  $J_{1,3} = 15.6$  Hz), 2.7 (s, 3H), 2.85 (t, 2H,  $J = 7.9$  Hz), 4.26 (dd, 2H,  $J_{1,2} = 3.8$  Hz,  $J_{1,3} = 14$  Hz), 4.58 (s, 2H), 5.27 (s, 2H), 6.83 (d, 2H,  $J = 8.5$  Hz), 6.98 (d, 2H,  $J = 8.3$  Hz), 7.02–7.11 (m, 3H).  $^{13}\text{C}$  NMR ( $\text{CDCl}_3$ , 100 MHz):  $\delta$  14.0, 14.1, 16.7, 21.8, 29.7, 46.5, 61.3, 65.4, 107.1, 115.1 (2C), 122.0, 122.45, 127.4 (2C), 129.1, 129.4, 134.9, 141.9, 154.5, 157.4, 168.6. HRMS: calcd for  $\text{C}_{22}\text{H}_{27}\text{N}_2\text{O}_3$  367.2022 [M + H], found 367.2018; mp 79.89 °C. IR: 3384, 2963, 2931, 2872, 1757, 1512  $\text{cm}^{-1}$ . UPLC (method 1): 95% pure (1.11 min). UPLC (method 2): 97% pure (0.61 min).

**Ethyl 2-Methyl-2-(4-((4-methyl-2-propyl-1H-benzimidazol-1-yl)methyl)phenoxy)propanoate (6).** Yield 26%.  $^1\text{H}$  NMR ( $\text{CDCl}_3$ , 400 MHz):  $\delta$  1.00 (t, 3H,  $J = 7.5$  Hz), 1.23 (t, 3H,  $J = 7.0$  Hz), 1.57 (s, 6H), 1.77 (dd, 2H,  $J_{1,2} = 7.6$  Hz,  $J_{1,3} = 15.6$  Hz), 2.7 (s, 3H), 2.85 (t, 2H,  $J = 7.8$  Hz), 4.21 (dd, 2H,  $J_{1,2} = 7.2$  Hz,  $J_{1,3} = 14$  Hz), 5.26 (s, 2H), 6.77 (d, 2H,  $J = 8.8$  Hz), 6.94 (d, 2H,  $J = 8.8$  Hz), 7.06 (m, 3H).  $^{13}\text{C}$  NMR ( $\text{CDCl}_3$ , 100 MHz):  $\delta$  14.0 (2C), 16.7, 21.8, 25.3 (2C), 29.7, 46.5, 61.4, 79.2, 107.0, 119.4 (2C), 122.0, 122.3, 127.1 (2C), 129.1, 129.7, 135.0, 141.9, 154.5, 155.0, 173.9. HRMS: calcd for  $\text{C}_{24}\text{H}_{31}\text{N}_2\text{O}_3$  395.2335 [M + H], found 395.2352. IR: 3384, 2959, 1724, 1609, 1509, 1142  $\text{cm}^{-1}$ . UPLC (method 1): 100% pure (1.85 min). UPLC (method 2): 100% pure (0.69 min).

**Ethyl 2,2-Dimethyl-3-(4-(2-(4-methyl-2-propyl-1H-benzimidazol-1-yl)ethoxy)phenyl)propanoate (8).** Yield 84%.  $^1\text{H}$  NMR ( $\text{CDCl}_3$ , 400 MHz):  $\delta$  1.10 (t, 3H,  $J = 7.3$  Hz), 1.14 (s, 6H), 1.23 (t, 3H,  $J = 7.3$  Hz), 1.94 (dd, 2H,  $J_{1,2} = 7.5$  Hz,  $J_{1,3} = 15.3$  Hz), 2.68 (s, 3H), 2.78 (s, 2H), 2.99 (t, 2H,  $J = 8.0$  Hz), 4.11 (dd, 2H,  $J_{1,2} = 7.0$  Hz,  $J_{1,3} = 14.1$  Hz), 4.24 (t, 2H,  $J = 5.7$  Hz), 4.51 (t, 2H,  $J = 5.5$  Hz), 6.71 (d, 2H,  $J = 8.8$  Hz), 7.00 (d, 2H,  $J = 8.5$  Hz), 7.05 (d, 1H,  $J = 7.0$  Hz), 7.13–7.21 (m, 2H).  $^{13}\text{C}$  NMR ( $\text{CDCl}_3$ , 100 MHz):  $\delta$  14, 14.1, 16.7, 20.9, 24.8 (2C), 29.5, 43.2, 43.4, 45.3, 60.3, 65.8, 106.6, 113.8 (2C), 121.9, 122.4, 129.3, 130.9, 131.1 (2C), 134.5, 142.1, 154.8, 156.7, 177.3. HRMS: calcd for  $\text{C}_{26}\text{H}_{35}\text{N}_2\text{O}_3$  423.2648 [M + H], found 423.2642. IR: 3386, 2967, 2932, 2872, 1724, 1610, 1511  $\text{cm}^{-1}$ . UPLC (method 1): 74% pure (0.57 min). UPLC (method 2): 93% pure (0.64 min).

**Ethyl 2-Methyl-3-(4-(2-(4-methyl-2-propyl-1H-benzimidazol-1-yl)ethoxy)phenyl)-2-phenoxypropanoate (9).** Yield 49%.  $^1\text{H}$  NMR ( $\text{CDCl}_3$ , 400 MHz):  $\delta$  1.12 (t, 3H,  $J = 7.3$  Hz), 1.23 (t, 3H,  $J = 7.0$  Hz), 1.40 (s, 3H), 1.95 (dd, 2H,  $J_{1,2} = 7.5$  Hz,  $J_{1,3} = 15.1$  Hz), 2.70 (s, 3H), 2.98–3.03 (m, 2H), 3.11 (d, 1H,  $J = 13.8$  Hz), 3.29 (d, 1H,  $J = 13.8$  Hz), 4.19–4.28 (m, 4H), 4.50–4.53 (t, 2H,  $J = 5.2$  Hz), 6.71 (d, 2H,  $J = 8.5$  Hz), 6.76 (d, 1H,  $J = 8.0$  Hz), 6.98–7.01 (m, 2H), 7.06 (d, 1H,  $J = 7.0$  Hz), 7.15–7.18 (m, 3H), 7.21–7.26 (m, 2H), 7.28 (s, 1H).  $^{13}\text{C}$  NMR ( $\text{CDCl}_3$ , 100 MHz):  $\delta$  14.0, 14.1, 16.7, 20.6, 22.0, 29.5, 43.2, 44.6, 53.4, 65.9, 81.9, 106.6, 113.9 (2C), 114.2, 119.3 (2C), 122.2, 128.4, 129.1 (2C), 129.3, 130.57, 131.8 (2C), 134.5, 142.1, 154.8, 155.4, 157.1, 173.6. HRMS: calcd for  $\text{C}_{31}\text{H}_{37}\text{N}_2\text{O}_4$  501.2753 [M + H], found

501.2729. IR: 2962, 2872, 1733, 1598, 1511, 1237  $\text{cm}^{-1}$ . UPLC (method 2): 100% pure (0.55 min). HPLC (method 3): 96.9% pure (1.42 min).

**Ethyl 3-(4-(2-(1,7'-Dimethyl-2'-propyl-1H,3'H-2,5'-bibenzimidazol-3'-yl)ethoxy)phenyl)-2-methyl-2-phenoxypropanoate (10).** Yield 30%.  $^1\text{H}$  NMR ( $\text{CDCl}_3$ , 400 MHz):  $\delta$  1.13 (t, 3H,  $J = 7.3$  Hz), 1.21 (t, 3H,  $J = 7.0$  Hz), 1.36 (s, 3H), 1.99 (dd, 2H,  $J_{1,2} = 7.5$  Hz,  $J_{1,3} = 15.3$  Hz), 2.75 (s, 3H), 3.02–3.08 (m, 3H), 3.25 (d, 1H,  $J = 13.8$  Hz), 3.90 (s, 3H), 4.19 (dd, 2H,  $J_{1,2} = 7.3$  Hz,  $J_{1,3} = 14.3$  Hz), 4.29 (t, 2H,  $J = 5.2$  Hz), 4.59 (t, 2H,  $J = 5.2$  Hz), 6.73 (d, 3H,  $J = 8.5$  Hz), 6.81 (d, 1H,  $J = 7.5$  Hz), 6.97 (t, 1H,  $J = 7.3$  Hz), 7.13 (d, 1H,  $J = 8.8$  Hz), 7.21 (t, 2H,  $J = 7.5$  Hz), 7.28 (s, 1H), 7.32–7.35 (m, 2H), 7.38–7.41 (m, 2H), 7.70 (s, 1H), 7.83–7.86 (m, 1H).  $^{13}\text{C}$  NMR ( $\text{CDCl}_3$ , 100 MHz):  $\delta$  14.0, 14.1, 16.8, 20.6, 21.8, 29.6, 31.9, 43.4, 44.6, 61.3, 65.9, 81.8, 108.5, 109.5, 113.9 (2C), 114.2, 119.3 (2C), 119.6, 122.3, 133.5, 123.8, 128.5, 129.1 (2C), 129.3, 130.5, 131.7 (2C), 134.7, 136.7, 143.0, 143.2, 154.8, 155.3, 156.8, 157.0, 173.6. HRMS: calcd for  $\text{C}_{39}\text{H}_{43}\text{N}_4\text{O}_4$  631.3284 [M + H], found 631.3275. IR: 3385, 2933, 1733, 1610, 1597, 1510, 1488  $\text{cm}^{-1}$ . UPLC (method 1): 96% pure (1.97 min). UPLC (method 2): 94% pure (1.83 min).

**3-(4-(2-(1,7'-Dimethyl-2'-propyl-1H,3'H-2,5'-bibenzimidazol-3'-yl)ethoxy)phenyl)-2-methyl-2-phenoxypropanoic acid (11).** Potassium hydroxide (50 mg) was added to a solution of **10** (15 mg, 0.016 mmol) in MeOH (5 mL). After stirring for 24 h at room temperature, the organic phase was evaporated under reduced pressure and pH was adjusted to 7. The aqueous layer was extracted with EtOAc. The organic layer was dried using  $\text{MgSO}_4$  and evaporated. The crude mixture was purified by silica gel column chromatography eluting with chloroform/methanol (9:1) and afforded 8 mg (88% yield) of **11**.  $^1\text{H}$  NMR (MeOH, 500 MHz):  $\delta$  1.09 (t, 3H,  $J = 7.5$  Hz), 1.25 (s, 3H), 1.94 (dd, 2H,  $J_{1,2} = 7.5$  Hz,  $J_{1,3} = 15.1$  Hz), 2.68 (s, 3H), 2.99–3.08 (m, 3H), 3.21 (d, 1H,  $J = 13.8$  Hz), 3.85 (s, 3H), 4.67 (t, 2H,  $J = 4.2$  Hz), 4.69 (t, 2H,  $J = 4.5$  Hz), 6.72 (d, 2H,  $J = 8.3$  Hz), 6.85–6.90 (m, 3H), 7.10–7.18 (m, 4H), 7.30–7.36 (m, 2H), 7.42 (s, 1H), 7.50–7.52 (m, 1H), 7.68–7.70 (m, 1H), 7.77 (s, 1H).  $^{13}\text{C}$  NMR (MeOH, 125 MHz): 12.9, 15.4, 20.0, 21.3, 28.7, 30.8, 43.3, 43.8, 66.0, 82.2, 109.4, 110.0, 113.5 (2C), 117.8, 118.8 (2C), 121.0, 122.5, 122.7, 122.9, 123.7, 128.5 (2C), 128.6, 129.3, 131.5 (2C), 134.3, 136.1, 141.3, 142.1, 154.4, 155.9, 157.0, 157.6, 158.61, 178.6. HRMS: calcd for  $\text{C}_{37}\text{H}_{39}\text{N}_4\text{O}_4$  603.2971 [M + H], found 603.2981. IR: 3385, 2925, 1577, 1458, 1225  $\text{cm}^{-1}$ . UPLC (method 1): 94% pure (1.72 min). UPLC (method 2): 93% pure (1.80 min).

Radioligand binding assays of  $\text{AT}_1$  receptors were carried out as described previously<sup>31</sup> using  $^{125}\text{I}$ -sar<sup>1</sup>ile<sup>8</sup> angiotensin II prepared as described previously.<sup>32</sup>

**Acknowledgment.** This investigation was conducted in a facility constructed with support from research facilities improvement program grant number C06 Rr-14503-01 from the National Center for Research Resources, National Institutes of Health. NIH grant 2R42AR44767-02A2 for Bethesda Pharmaceuticals is also acknowledged for the partial support.

**Supporting Information Available:** Procedures and characterization data for all the intermediate compounds; procedures for biochemical assays and computational methods. This material is available free of charge via the Internet at <http://pubs.acs.org>.

## References

- (1) Grundy, S. M.; Brewer, H. B., Jr.; Cleeman, J. I.; Smith, S. C., Jr.; Lenfant, C. Definition of metabolic syndrome: Report of the National Heart, Lung, and Blood Institute/American Heart Association conference on scientific issues related to definition. *Circulation* **2004**, *109*, 433–438.
- (2) Ford, Earl, S. Risks for all-cause mortality, cardiovascular disease, and diabetes associated with the metabolic syndrome: a summary of the evidence. *Diabetes Care* **2005**, *28*, 1769–1778.

- (3) Cameron, A. J.; Shaw, J. E.; Zimmet, P. Z. The metabolic syndrome: prevalence in worldwide populations. *Endocrinol. Metab. Clin. North Am.* **2004**, *33*, 351–375, Table of Contents.
- (4) Zimmet, P.; Alberti, K. G. M. M.; Shaw, J. Global and societal implications of the diabetes epidemic. *Nature (London)* **2001**, *414*, 782–787.
- (5) Morphy, R.; Kay, C.; Rankovic, Z. From magic bullets to designed multiple ligands. *Drug Discovery Today* **2004**, *9*, 641–651.
- (6) Edwards, I. R.; Aronson, J. K. Adverse drug reactions: definitions, diagnosis, and management. *Lancet* **2000**, *356*, 1255–1259.
- (7) Morphy, R.; Rankovic, Z. The Physicochemical Challenges of Designing Multiple Ligands. *J. Med. Chem.* **2006**, *49*, 4961–4970.
- (8) Morphy, R.; Rankovic, Z. Designed Multiple Ligands. *J. Med. Chem.* **2005**, *48*, 6523–6543.
- (9) Rubenstrunk, A.; Hanf, R.; Hum, D. W.; Fruchart, J.-C.; Staels, B. Safety issues and prospects for future generations of PPAR modulators. *Biochim. Biophys. Acta, Mol. Cell Biol. Lipids* **2007**, *1771*, 1065–1081.
- (10) Inguibert, N.; Poras, H.; Teffo, F.; Beslot, F.; Selkti, M.; Tomas, A.; Scalbert, E.; Bennejean, C.; Renard, P.; Fournie-Zaluski, M.-C.; Roques, B.-P. N-2-(Indan-1-yl)-3-mercapto-propionyl amino acids as highly potent inhibitors of the three vasopeptidases (NEP, ACE, ECE): in vitro and in vivo activities. *Bioorg. Med. Chem. Lett.* **2002**, *12*, 2001–2005.
- (11) Flynn, G. A.; Beight, D. W.; Mehdi, S.; Koehl, J. R.; Giroux, E. L.; French, J. F.; Hake, P. W.; Dage, R. C. Application of a conformationally restricted Phe-Leu dipeptide mimetic to the design of a combined inhibitor of angiotensin I-converting enzyme and neutral endopeptidase 24.11. *J. Med. Chem.* **1993**, *36*, 2420–2423.
- (12) Robl, J. A.; Sun, C.-Q.; Stevenson, J.; Ryono, D. E.; Simpkins, L. M.; Cimarusti, M. P.; Dejneka, T.; Slusarchyk, W. A.; Chao, S.; Stratton, L.; Misra, R. N.; Bednarz, M. S.; Asaad, M. M.; Cheung, H. S.; Abboa-Offei, B. E.; Smith, P. L.; Mathers, P. D.; Fox, M.; Schaeffer, T. R.; Seymour, A. A.; Trippodo, N. C. Dual Metalloprotease Inhibitors: Mercaptoacetyl-Based Fused Heterocyclic Dipeptide Mimetics as Inhibitors of Angiotensin-Converting Enzyme and Neutral Endopeptidase. *J. Med. Chem.* **1997**, *40*, 1570–1577.
- (13) Xu, Y.; Rito, C. J.; Etgen, G. J.; Ardecky, R. J.; Bean, J. S.; Bensch, W. R.; Bosley, J. R.; Broderick, C. L.; Brooks, D. A.; Dominianni, S. J.; Hahn, P. J.; Liu, S.; Mais, D. E.; Montrose-Rafizadeh, C.; Ogilvie, K. M.; Oldham, B. A.; Peters, M.; Rungta, D. K.; Shuker, A. J.; Stephenson, G. A.; Tripp, A. E.; Wilson, S. B.; Winneroski, L. L.; Zink, R.; Kauffman, R. F.; McCarthy, J. R. Design and Synthesis of  $\alpha$ -Aryloxy- $\alpha$ -methylhydrocinnamic Acids: A Novel Class of Dual Peroxisome Proliferator-Activated Receptor  $\alpha/\gamma$  Agonists. *J. Med. Chem.* **2004**, *47*, 2422–2425.
- (14) Henke, B. R. Peroxisome Proliferator-Activated Receptor  $\alpha/\gamma$  Dual Agonists for the Treatment of Type 2 Diabetes. *J. Med. Chem.* **2004**, *47*, 4118–4127.
- (15) Benson, S. C.; Pershadsingh, H. A.; Ho, C. I.; Chittiboyina, A.; Desai, P.; Pravenec, M.; Qi, N.; Wang, J.; Avery, M. A.; Kurtz, T. W. Identification of Telmisartan as a Unique Angiotensin II Receptor Antagonist With Selective PPAR $\gamma$ -Modulating Activity. *Hypertension* **2004**, *43*, 993–1002.
- (16) Chittiboyina, A. G.; Mizuno, C. S.; Desai, P. V.; Patny, A.; Kurtz, T. W.; Pershadsingh, H. A.; Speth, R. C.; Karamyan, V.; Avery, M. A. Design, synthesis, and docking studies of novel telmisartan–glitazone hybrid analogs for the treatment of metabolic syndrome. *Med. Chem. Res.* **2009**, *18*, 589–610.
- (17) Mizuno, C. S.; Chittiboyina, A. G.; Patny, A.; Kurtz, T. W.; Pershadsingh, H. A.; Speth, R. C.; Karamyan, V. T.; Avery, M. A. Design, synthesis, and docking studies of telmisartan analogs for the treatment of metabolic syndrome. *Med. Chem. Res.* **2009**, 611–628.
- (18) Chakravarty, P. K.; Patchett, A. A.; Camara, V. J.; Walsh, T. F.; Greenlee, W. J. Preparation and formulation of benzimidazoles as angiotensin II antagonists. Patent 90-305179 400835, 19900514, **1990**.
- (19) Larhed, M.; Hallberg, A. Microwave-Promoted Palladium-Catalyzed Coupling Reactions. *J. Org. Chem.* **1996**, *61*, 9582–9584.
- (20) Steggles, D. J.; Verge, J. P. Pharmaceutical ethanone compounds. Patent 84-304759 132124, 19840712, **1985**.
- (21) Santhosh, K. C.; Paul, G. C.; De Clercq, E.; Pannecouque, C.; Witvrouw, M.; Loftus, T. L.; Turpin, J. A.; Buckheit, R. W., Jr.; Cushman, M. Correlation of anti-HIV activity with anion spacing in a series of cosalane analogs with extended polycarboxylate pharmacophores. *J. Med. Chem.* **2001**, *44*, 703–714.
- (22) Brooks, D. A.; Godfrey, A. G.; Jones, S. B.; McCarthy, J. R.; Rito, C. J.; Winneroski, L. L., Jr.; Xu, Y. Preparation of oxazolyl-arylpropionic acid derivatives and their use as PPAR agonists. Patent 2001-US22616 2002016331, 20010823, **2002**.
- (23) Patny, A.; Desai, P. V.; Avery, M. A. Ligand-supported homology modeling of the human angiotensin II type 1 (AT1) receptor: insights into the molecular determinants of telmisartan binding. *Proteins: Struct., Funct., Bioinf.* **2006**, *65*, 824–842.
- (24) Balmforth, A. J.; Lee, A. J.; Warburton, P.; Donnelly, D.; Ball, S. G. The conformational change responsible for AT1 receptor activation is dependent upon two juxtaposed asparagine residues on transmembrane helices III and VII. *J. Biol. Chem.* **1997**, *272*, 4245–4251.
- (25) Hoe, K.-L.; Saavedra, J. M. Site-directed mutagenesis of the gerbil and human angiotensin II AT1 receptors identifies amino acid residues attributable to the binding affinity for the nonpeptidic antagonist losartan. *Mol. Pharmacol.* **2002**, *61*, 1404–1415.
- (26) Ries, U. J.; Mihm, G.; Narr, B.; Hasselbach, K. M.; Wittneben, H.; Entzeroth, M.; van Meel, J. C.; Wienen, W.; Huel, N. H. 6-Substituted benzimidazoles as new nonpeptide angiotensin II receptor antagonists: synthesis, biological activity, and structure-activity relationships. *J. Med. Chem.* **1993**, *36*, 4040–51.
- (27) Nolte, R. T.; Wisely, G. B.; Westin, S.; Cobb, J. E.; Lambert, M. H.; Kurokawa, R.; Rosenfeld, M. G.; Willson, T. M.; Glass, C. K.; Milburn, M. V. Ligand binding and co-activator assembly of the peroxisome proliferator-activated receptor- $\gamma$ . *Nature* **1998**, *395*, 137–143.
- (28) Lemberger, T.; Desvergne, B.; Wahli, W. Peroxisome proliferator-activated receptors: a nuclear receptor signaling pathway in lipid physiology. *Annu. Rev. Cell Dev. Biol.* **1996**, *12*, 335–363.
- (29) Goebel, M.; Clemenz, M.; Staels, B.; Unger, T.; Kintscher, U.; Gust, R. Characterization of new PPAR $\gamma$  agonists: analysis of telmisartan's structural components. *ChemMedChem* **2009**, *4*, 445–456.
- (30) Tagami, T.; Yamamoto, H.; Moriyama, K.; Sawai, K.; Usui, T.; Shimatsu, A.; Naruse, M. A selective peroxisome proliferator-activated receptor- $\gamma$  modulator, telmisartan, binds to the receptor in a different fashion from thiazolidinediones. *Endocrinology* **2009**, *150*, 862–870.
- (31) Speth, R. C. Sarcosine1, glycine8 angiotensin II is an AT1 angiotensin II receptor subtype selective antagonist. *Regul. Pept.* **2003**, *115*, 203–209.
- (32) Speth, R. C.; Harding, J. W. Radio labeling of angiotensin peptides. *Methods Mol. Med.* **2001**, *51*, 275–295.